

Multi-Person Pose Regression via Pose Filtering and Scoring

Huixin Miao

Dalian University of Technology

Junqi Lin

Dalian University of Technology

Junjie Cao*

Dalian University of Technology

Abstract

Multi-person pose estimation is one of the mainstream tasks of computer vision. Existing methods include the top-down methods which need additional human detector and the bottom-up methods which need to complete heuristic grouping after predicting all human keypoints. They all need to deal with the grouping and detection of keypoints separately, resulting in low efficiency. In this work, we propose an end-to-end network framework for multi-person pose regression to predict the instance-aware keypoints directly. This framework uses a cascaded manner: the first stage provides basic estimation. Then we propose the OKS-Filter which is used to remove low-quality predictions, so that the second stage could focus on better results for further optimization. In addition, in order to quantify the quality of the predicted poses, we also propose the pose scoring module (PSM), so that when using non-maximum suppression (NMS) in the inference, the correct type and high-quality poses are preserved. We have verified on the COCO keypoint benchmark. The experiments show that our multi-person pose regression network is feasible and effective, and the two newly proposed modules are helpful to improve the performance of the model.

1. Introduction

Multi-person pose estimation is to identify and locate all keypoints of different people from a single image. It is one of the basic tasks in computer vision and is extremely challenging. It is widely used in motion recognition, pedestrian tracking and 3D human pose estimation, etc.

Existing methods are roughly divided into top-down and bottom-up methods. The top-down method[3, 6, 4, 21, 24, 22] first uses an independent human detector to detect all the people in the image, and then crops the corresponding area to perform a single human pose estimation. Because the human detector and the pose estimation require two different neural networks, it causes great computational

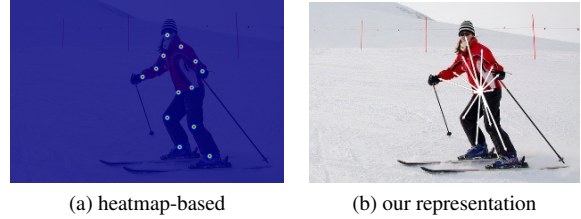


Figure 1: (a) is based on the heatmap, (b) is our pose representation. Our method directly predicts structured poses of multiple people. Compared with the heatmap-based method, we omit the step of composing keypoints into different people.

overhead. Moreover, the running time heavily depends on the number of people in the image. As for the bottom-up method[2, 11, 15, 19, 18], first detect all identity-free keypoints, and then assign them to corresponding people. Because there is no clear semantic connection between keypoints, it is extremely difficult to assign them accurately. Therefore, the above two heatmap-based methods need to convert the generated keypoints, resulting in a relatively long process.

In order to overcome the above limitations, we use a cascaded manner to predict the relative distance between keypoints and the center of gravity of the human body in the first stage and gradually refine predictions in the second stage, as shown in Fig.1. However, the performance obtained is not satisfactory. The main reason is that some poses generated in the first stage which are far away from ground truth are still sent to the second stage for refining. Based on this situation, we propose the OKSFilter to remove those low-quality poses, so that the network only learns through high-quality poses, thereby improving the performance of the entire model. Among them, OKS(Object Keypoint Similarity) is used to evaluate the similarity between the predicted pose and the true value.

Classification score is used to evaluate whether there is a person at the corresponding position in the image. Since

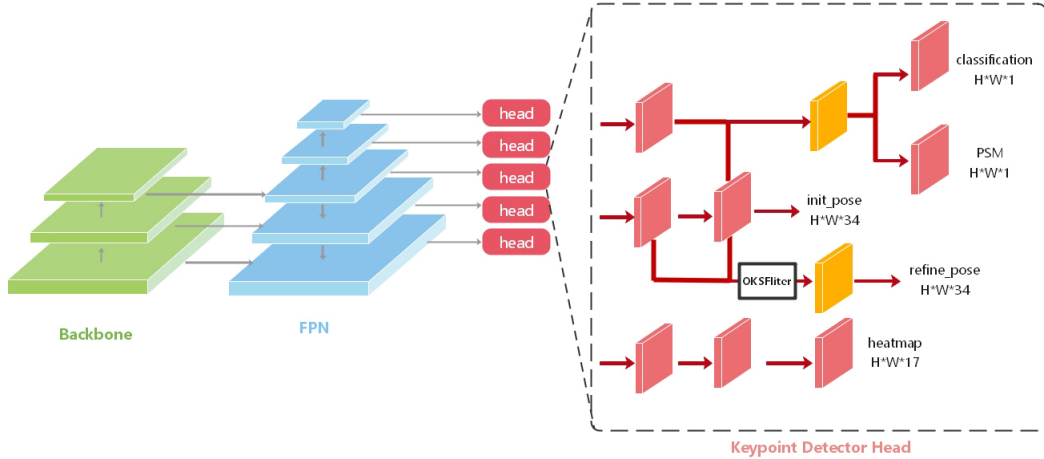


Figure 2: Our network framework for end-to-end multi-person pose estimation. C3, C4, and C5 are the feature maps of the backbone network, and from P3 to P7 are the feature maps of the feature pyramid network. In the head, red indicates normal convolution, and orange indicates deformable convolution. The classification is used to indicate whether there is a person in the corresponding position in the feature map, and PSM is used to score the predicted the final pose. The initial pose passes OKSFilter to generate a refined pose through deformable convolution. Heatmap is used to assist the network to learn the location of keypoints.

the classification score and the quality of pose are not completely positively correlated[10], pixels with high classification scores may correspond to a low-quality pose, so we propose PSM to learn the OKS metric between the predicted pose and ground truth. In the inference, using the scores learned from PSM to weight the classification scores, a pose of both correct type and high quality can be preserved.

Compared with the top-down and bottom-up methods, the method proposed in this paper has the following advantages.

- We propose an end-to-end network that does not require pre-processing of human detection nor post-processing of grouping, which greatly improves operating efficiency.
- During training, we propose the OKSFilter to make the network pay more attention to high-quality poses. During inferring, we proposed PSM to obtain the pose of both correct type and high quality.
- Our proposed method is based on regression, which can directly predict the precise coordinates of keypoints. Unlike the heatmap-based method, it can avoid quantization errors during downsampling.

2. Related Work

Top-down Methods. The top-down method[3, 6, 4, 21, 16, 3, 22] performs single-person pose estimation in the bounding box obtained by a human detector. Newell et al.[16] propose a stacked hourglass network to complete feature extraction through repeated up and down sampling.

Chen et al.[3] propose a cascaded pyramid network, using cascading methods to focus on the keypoints that are difficult to learn, which is similar to our method, but they need to first generate a bounding box, and then predict the keypoints by using heatmaps. We directly predict the precise coordinates of keypoints through dense prediction. Sun et al.[22] propose a high-resolution network to maintain high-resolution representations through the whole process.

Bottom-up Methods. The bottom-up method[2, 11, 15, 23] first predicts all identity-free keypoints and then groups them heuristically. Cao et al. [2] propose to use part affinity field to establish connections between keypoints. Then they use the greedy algorithm to combine the corresponding keypoints with the highest scores. Newell et al.[15] use stacked hourglass network as the backbone network to generate keypoints, and propose to group keypoints by associate embedding. They generate a tag for each keypoint, and keypoints with the same tag belong to the same person. Sun et al.[23] propose to use HigherHRNet to generate heatmaps of different resolutions and combine them to generate keypoints. And then they use associate embedding proposed in [15] to group keypoints.

Single-Stage Multi-Person Pose Estimation. Nie et al.[17] proposed SPM, the first single-stage model. They predict heatmap for root joint and dense displacement maps for body joints. Therefore, they need a complex group post-processing to combine all the keypoints into different

people. But we directly predicted the instance-aware keypoints, eliminating the above-mentioned post-processing operations.

Anchor-free Object Detectors. The anchor-free object detector uses some points in the image as training samples to generate the final bounding box. Tian et al.[27] propose to use the points in the ground truth as training samples, and then use "center-ness" to suppress low-quality bounding boxes. Conceptually, they use the training sample to generate two points, namely the left-top and right-bottom points of the bounding box, and we expand it to generate N keypoints, use it as a basic network framework, and make improvements to better solve the multi-person pose estimation problem. Yang et al.[28] use center points proposed in YOLO[20] to generate some representative points first, and then use deformable convolution to align features to generate the final bounding box. We will draw on this method to complete the alignment of human pose and features.

3. Our Approach

In this section, we first introduce the pose representation used in this paper. Next, we show the OKSFilter we proposed to remove some low-quality detected poses. Finally, we present our proposed PSM to quality detected poses and preserve the correct type and high-quality poses.

3.1. OKSFilter

The pose of the human body can be expressed as a series of coordinates of keypoints, namely:

$$P = \{p_i^1, p_i^2, \dots, p_i^k\}_{i=1}^N \quad (1)$$

$$p_i^j = (x_i^j, y_i^j) \quad (2)$$

Where P represents the set of all human poses in the image, k represents the number of keypoints, and N represents the number of people in the image. p_i^j represents the 2D coordinate of the j th keypoint of the i th person.

This paper uses structured representation to represent keypoints as the coordinates of the center point of the human body and the relative displacement of other keypoints to the center point. Then the j th keypoint of the i th person can be expressed as:

$$(x_i^j, y_i^j) = (x_i^c, y_i^c) + (\Delta x_i^j, \Delta y_i^j) \quad (3)$$

where (x_i^c, y_i^c) represents the center point of the i th person and $(\Delta x_i^j, \Delta y_i^j)$ represents the relative displacement. Thus, the pose of multiple people is represented as a set of center points and offsets:

$$P = \{(x_i^c, y_i^c), (\Delta x_i^1, \Delta y_i^1), \dots, (\Delta x_i^k, \Delta y_i^k)\}_{i=1}^N \quad (4)$$

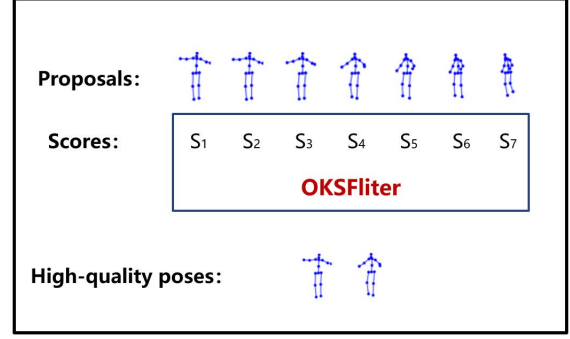


Figure 3: Specific diagram of OKSFilter. First, use OKS to evaluate the similarity between the proposal and the ground truth to obtain the score S_i for proposal, and then select the high quality proposal for the next stage of refinement.

The structured representation method effectively encodes the pose of the human body, which helps us to make dense prediction.

Many of the initial poses generated in the first stage of RefineNet are far from the ground truth. If these poses are sent to the second stage, the network will not be able to concentrate on high-quality poses and affect the classification of training samples. At the same time, it also increases a lot of unnecessary calculations.

For the above reasons, we propose OKSFilter to solve these problems, as shown in Fig.3. Suppose that N poses were generated in the initial stage. OKSFilter first converts the representation of these N poses from formula (4) to formula (1). Then calculate the similarity between each pose and the M ground truth in the image (for the calculation formula of similarity, see Section 3.2), and take the maximum value as the score of this pose. Through the above method, the score of each initial pose is obtained. Then, OKSFilter screens all poses through a hyperparameter threshold. Poses above the threshold are retained and sent to the second stage, and poses below the threshold are removed. It is proved by experiments that after OKSFilter, the performance of the model has been further improved.

3.2. PSM

We first use the center-ness branch proposed in FCOS to weight the classification score, which is used to remove the low-quality predicted poses produced by locations far away from the human body. However, the center-ness score only focuses on whether the position is in the center of the human body, but not on the quality of the generated pose. Therefore, in order to be more suitable for the problem of multi-person pose estimation, we replaced it with PSM to score the quality of each pose.

We use OKS to measure the similarity between the predicted pose and the ground truth. The specific formula is as

follows:

$$OKS = \frac{\sum_i e^{\frac{-d_i^2}{2s^2\kappa_i^2}} \delta(v_i > 0)}{\sum_i [\delta(v_i > 0)]} \quad (5)$$

The d_i are the Euclidean distances between each corresponding ground truth and predicted keypoint and the v_i are the visibility flags of the ground truth. s is the object scale and κ_i is a per-keypoint constant that controls falloff.

OKS is a number in the range of 0 to 1. During training, we use the maximum value of OKS for each pose to weight the loss function. Thus, the predicted pose of high OKS gets higher loss weight, and the predicted pose of low OKS gets lower loss weight. As a result, the network better learns high-quality poses and ignores low-quality poses to some extent. Moreover, this method adaptively learns the pose without setting any hyperparameters.

When testing, we use PSM to weight the classification scores, that is, the product of the classification score and the pose score is used as the confidence of each final pose, so that by the NMS process, the correct type and high-quality poses are preserved. Experimental results show that PSM has better performance than the center-ness.

4. Our End-to-End Framework

We use ResNet[9] or HRNet[22] as the backbone network, and then use the feature pyramid network(FPN)[12] to generate multi-scale features to solve the problem of human body scale changes. And the prediction head is shared between features of different scales, as shown in Fig.2. Heads include classification branch, regression branch which are used for different layer features of the feature pyramid(P_3, P_4, P_5, P_6, P_7) and a separate heat map branch. The downsampling rates of these features relative to the input image are 8, 16, 32, 64, and 128, respectively. For the classification branch, the number of output channels is 1, which is a binary classification discriminator, used to determine whether it is the center point of the human body in the image. The number of output channels of the regression branch is $2K$ (K represents the number of keypoints), which represents the offset of the human keypoints relative to this position. We refer to the above network framework as a baseline. However, its performance is poor. In order to further optimize the output results, we adopt a cascading approach to treat the current output as a candidate pose, and then use our proposed OKSFilter and feature alignment for further refinement to get the final pose. And we also use the PSM we proposed, its output channel is also 1, used to score the predicted pose.

Center Sampling. For each position (x, y) on the feature map, it can be mapped back to the corresponding position $(xs + \lfloor \frac{s}{2} \rfloor, ys + \lfloor \frac{s}{2} \rfloor)$ on the original image. This position is the center of the receptive field of the feature. If

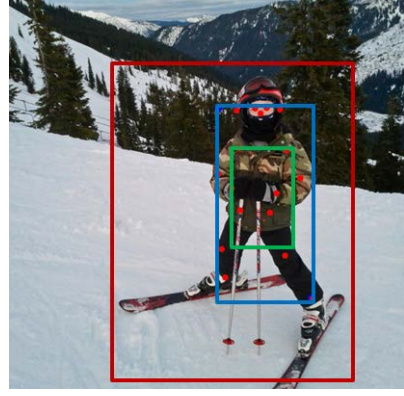


Figure 4: The specific implementation of center sampling. In the figure, red represents the bounding box of the person, blue represents the smallest pseudo box that surrounds all keypoints, and green represents the bounding box obtained after applying central sampling. It can be seen that the positions enclosed by the green bounding box are almost all on the human body, and the poses generated from these positions are more meaningful. And this way will not affect the learning of the classifier.

the coordinates of the original image corresponding to the position (x, y) on the feature map fall within the bounding box surrounding the human body, it is regarded as a positive sample, this point is assigned a label of 1, and the relative offset is calculated; Otherwise, it is regarded as a negative sample, label 0 is assigned, and the offset is not calculated. It is verified through experiments that although the above method alleviates the imbalance of positive and negative samples to a certain extent, it will bring more positive samples of low quality and reduce the performance. Combined with the human body pose representation method, in theory, only the human body center point needs to be taken as a positive sample. However, too few positive samples are generated in this way, which is not conducive to the training of the classifier. Therefore, we first replace the bounding box with the smallest pseudo box surrounding all key points, and then, the center point of the human body is amplified from a point to a small rectangular area surrounding the center point. The points in the rectangular area are regarded as positive samples. Other points are regarded as negative samples, as shown in Fig.4. It not only solves the problem of sample imbalance, but also ensures the performance of the regressor.

Feature Align. It is extremely difficult to decode all possible human poses through the unique feature vector corresponding to the current position. Because once the position of a keypoint in the image is far from the center of the receptive field corresponding to the feature, the response of the depth feature to the signal will quickly decay, so the

human pose must be aligned with the depth feature, otherwise the information in it cannot be decoded. Therefore, we propose an adaptive pose feature alignment module, which first performs feature acquisition and positioning, and then performs feature alignment. The specific expression is as follows:

$$L = \text{Sample}(P) \quad (6)$$

$$F^* = \text{Align}_{reg}(F, L) \quad (7)$$

where P represents the candidate's pose, L represents the feature sampling position, F represents the original feature, and F^* represents the aligned feature.

Heatmap. Due to the difficulty of training the regression branch[7, 25], we introduced heatmap[26] to assist. The heatmap branch is essentially a classification branch that classifies keypoint types. Suppose there are k types of keypoints, i is an integer in the range of 1 to k , the value of the point corresponding to the i -th keypoint on the feature map is i , if the point does not belong to any keypoint, the value is 0. During inference, the heatmap branch is not used, so no extra calculation is added. The heatmap branch only acts on the P_3 layer features, because the downsampling rate of other layers is large, and the keypoints will overlap the same position on the feature map, resulting in ambiguity.

Loss Function. Since the training samples on the feature map are mostly negative samples, so there is a serious imbalance problem. Therefore, for the classification branch and the heatmap branch, we use focal loss[13] as the loss function.

$$FL(p_t) = -(1 - p_t)^\gamma \log(p_t) \quad (8)$$

Where p_t is the predicted probability and γ is the hyper-parameter. For the regression branch, we use Smooth L1 loss[5] as the loss function. For PSM, we use binary cross entropy (BCE) loss as the loss function. The loss function of the entire network is as follows:

$$L = \lambda_1 L_{cls} + \lambda_2 L_{hm} + \lambda_3 L_{reg} + \lambda_4 L_{PSM} \quad (9)$$

5. Experiments

5.1. Implementation

Our experiments are conducted on the multi-person pose estimation task in the large-scale benchmark MS COCO dataset[14]. It contains more than 130,000 images and 250,000 person instances, each of which contains 17 keypoint annotations. Following the common practice[2, 8], we use 57,000 images for training, 5,000 images as validation for our ablation study and 20,000 images on the test-dev set to compare with other methods. The evaluation uses Average Precision (AP) based on OKS.

Training. We first adjust the size of the image to

800x1333, then randomly flip it with a probability of 0.5, and then crop it into 800x800 patches to complete the data augmentation.

We use stochastic gradient descent(SGD) optimizer. The initial learning rate is set to 0.0025, weight decay and momentum are set as 0.0001 and 0.9, respectively. The batch size is set to 8, and a total of 24 epochs are trained for ablation study and for the test-dev set to verify the feasibility of the proposed method.

Testing. When testing, the image size is also adjusted to 800x1333, and the prediction is made directly on the entire image. Firstly, according to the classification score, the positions of possible human bodies are screened. Then, the predicted human pose is used to generate a pseudo box that tightly surrounds the predicted keypoints of the human body. Finally, soft-nms[1] is used to eliminate redundant human poses to obtain the final prediction result.

5.2. Ablation Experiments

5.2.1 Basic network framework

	AP	AP^{50}	AP^{75}	AP^M	AP^L
Baseline	41.6	72.3	44.8	38.7	50.5
+ Align	48.3	77.2	51.6	42.1	57.2
+ Sampling	53.1	80.4	57.5	46.0	62.7
+ Heatmap	55.4	82.1	60.0	49.1	64.0

Table 1: Ablation experiments on COCO minival for basic network framework. "+ Align": using feature alignment to generate refined poses. "+ Sampling": using center sampling to adjust the distribution of positive and negative samples. "+ Heatmap": Use heatmap to assist training.

Baseline. First, we trained a simple basic model to verify that the fully convolutional neural network can use dense prediction to solve the multi-person pose estimation problem. The number of regression branch channels is 2k, which directly predicts the offset vector of k keypoints relative to the current position. Record this as the baseline. As shown in Table 1, the performance of the baseline is very low (41.6 mAP). Although good performance is obtained when the threshold is low(72.3 mAP when OKS=0.5), the performance decays rapidly when the threshold is high(44.8 mAP when OKS=0.75). Therefore, the results of the previous stage should be refined by cascading.

Feature Align. In this experiment, we use the proposed adaptive feature alignment module based on the baseline. We regard the output generated by the baseline as the proposed pose and use it as the input of the adaptive feature

	+ centerness	+ PSM	using centerness	using PSM	AP	AP^{50}	AP^{75}	AP^M	AP^L
Ours	✓		✓		58.7	82.7	65.3	52.4	67.5
Ours	✓	✓	✓		58.5	82.8	65.1	52.1	67.5
Ours	✓	✓		✓	59.2	82.9	65.9	52.8	68.2
Ours		✓		✓	60.5	82.9	66.6	54.1	69.3

Table 2: Ablation experiments on COCO minival for our proposed PSM. ”+ centerness”: using the centerness branch during training. ”+ PSM”: using the PSM branch during training. ”using centerness”:using the centerness branch during testing. ”using PSM”:using the PSM branch during testing.

alignment module. From Table 1, we can see that the performance of the model has been greatly improved (from 41.6 mAP to 48.3 mAP).

Center Sampling. The initial sample allocation method used in the experiment regards all positions corresponding to the human body’s bounding box as positive samples. Due to the effect of the effective receptive field, we only take a part of the area near the center point of the human body as a positive sample, and other areas as negative samples. The experimental results in Table 1 show the effectiveness of the center sampling (from 48.3 mAP to 53.1 mAP).

Heatmap. As shown in Table 1, the performance of the model has been improved by using heatmap for auxiliary supervision during training. As shown in Table 1, the performance is improved by 2.3 mAP. However, our model does not use heatmap as the prediction result during inference, which is different from other heatmap-based methods.

5.2.2 OKSFliter

As mentioned before, OKSFilter can filter out some low-quality poses generated in the initial stage, so that the network only learns through high-quality poses, thereby improving the performance of the entire model. We set the OKS threshold to 0.5, that is, when the OKS of the pose predicted in the initial stage is less than 0.5, it will not be sent to the next stage for refinement. As shown in Table 3, the performance was improved from 56.7 mAP to 58.7 mAP.

5.2.3 PSM

PSM is used to score the final predicted pose. Multiply the classification score and pose score to get the final score for each pose. As shown in Table 2, we initially trained the center-ness branch, and then used the center-ness score to weight the classification score. The result of 58.7mAP was obtained. Then we simply add the PSM branch during training without using it, and the final result drops by 0.2 mAP, because this method only adds one more item to the

loss function. Next, we replaced the center-ness with PSM during testing, which is to use the pose score to weight the classification score. It can be found that the final result has been increased from 58.5mAP to 59.2mAP. Theoretically, the center-ness branch and the PSM branch have similar functions, both of which weight the classification scores. Therefore, we replace center-ness with PSM during training and use only PSM during testing. It can be seen from Table 2 that it obtained the best result (60.5 mAP).

	AP	AP^{50}	AP^{75}	AP^M	AP^L
Baseline*	56.7	82.6	62.0	50.3	65.9
+ OKSFilter	58.7	82.7	65.3	52.4	67.5
+ PSM	60.5	82.9	66.6	54.1	69.3

Table 3: Ablation experiments on COCO minival for our proposed OKSFilter and PSM. ”Baseline*”: Increase the number of experimental epochs from 24 to 31. ”+ OKSFilter”:filter out some of the low-quality poses that are generated in the initial stage. ”+ PSM”: Learn the quality of each generated pose and use it to weight the classification score.

5.3. Comparison with State-of-the-art Methods

We compare our method with other state-of-the-art multi-person pose estimation methods on test-dev split of MS-COCO benchmark. When testing, neither flipped images nor multi-scale tests were used. The results are shown in Table 4. The network proposed in this paper obtains 60.0 mAP when using ResNet-50 as the backbone network, 60.8 mAP when using ResNet-101 as the backbone network, and 63.6 mAP when using HRNet-w32 as the backbone network.

Compared with the top-down method, the performance of our method exceeds Mask-RCNN (63.6 mAP vs. 62.7 mAP). Although compared with other top-down methods, the performance of our model is still lagging behind, but these models often require additional human detectors to obtain the human body’s bounding box, then crop and zoom, and then complete single-person pose estimation. And when the detected bounding boxes overlap, this

Method	AP	AP^{50}	AP^{75}	AP^M	AP^L	Times[s]
Mask-RCNN[8]	62.7	87.0	68.4	57.4	71.1	0.2
CPN[3]	72.1	91.4	80.0	68.7	77.2	-
RMPE[4]	72.3	89.2	79.1	68.0	78.6	-
HRNet[22]	75.5	92.5	83.3	71.9	81.5	-
AE[15]	56.6	81.8	61.8	49.8	67.0	0.25
CMU-Pose[2]	61.8	84.9	67.5	57.1	68.2	0.6
PersonLab[18]	65.5	87.1	71.4	64.1	75.5	0.464
Ours(R50)	60.0	84.5	66.4	53.6	68.5	0.063
Ours(R101)	60.8	84.7	67.3	54.3	69.5	0.083
Ours(HRNet-w32)	63.6	85.9	70.4	58.1	71.2	0.21

Table 4: Comparison with state-of-the-art methods on MS COCO test-dev dataset.

method is still calculated separately, so the speed is very slow. And we use the dense prediction method, the running time does not depend on the number of people in the image.

Compared with the bottom-up method, our method outperforms CMU-Pose[2](63.6 mAP vs. 61.8 mAP). And also achieved better performance than AE[15] (63.6 mAP vs. 56.6mAP).At the same time, our method does not require complicated post-processing such as heuristic grouping, which is simpler than the bottom-up algorithm and the test time is shorter. Moreover, the training time required by our algorithm is also shorter.

Timing. Our method on the test-dev set, the average inference time when using ResNet-50 as the backbone network is 0.06s, which is much faster than the Mask-RCNN[8] (0.2s) that takes the time advantage in the top-down methods, and much faster than CMU-Pose[2] (0.6s) that takes the time advantage in the bottom-down methods. Our method can provide ideas for real-time multi-person pose detection in industry.

6. Conclusion

In this paper, we study the method of human pose estimation based on object detection. The full convolutional neural network was used to make dense predictions. The network can be trained end-to-end, and through the structure-based pose representation method, it can be free from cumbersome post-processing steps, and has obvious advantages in speed. And our proposed OKSFilter and PSM significantly improve the performance of the algorithm. Finally, we demonstrate the effectiveness of the method proposed in this paper through detailed experiments.

References

- [1] N. Bodla, B. Singh, R. Chellappa, and L. S. Davis. Soft-nms—improving object detection with one line of code. In *Proceedings of the IEEE international conference on computer vision*, pages 5561–5569, 2017.
- [2] Z. Cao, T. Simon, S.-E. Wei, and Y. Sheikh. Realtime multi-person 2d pose estimation using part affinity fields. In *Proceedings of the IEEE Conference on Computer Vision and Pattern Recognition*, pages 7291–7299, 2017.
- [3] Y. Chen, Z. Wang, Y. Peng, Z. Zhang, G. Yu, and J. Sun. Cascaded pyramid network for multi-person pose estimation. In *Proceedings of the IEEE conference on computer vision and pattern recognition*, pages 7103–7112, 2018.
- [4] H.-S. Fang, S. Xie, Y.-W. Tai, and C. Lu. Rmpe: Regional multi-person pose estimation. In *Proceedings of the IEEE International Conference on Computer Vision*, pages 2334–2343, 2017.
- [5] R. Faster. Towards real-time object detection with region proposal networks. *Advances in neural information processing systems*, page 9199, 2015.
- [6] G. Gkioxari, B. Hariharan, R. Girshick, and J. Malik. Using k-poselets for detecting people and localizing their keypoints. In *Proceedings of the IEEE Conference on Computer Vision and Pattern Recognition*, pages 3582–3589, 2014.
- [7] X. Glorot and Y. Bengio. Understanding the difficulty of training deep feedforward neural networks. In *Proceedings of the thirteenth international conference on artificial intelligence and statistics*, pages 249–256, 2010.
- [8] K. He, G. Gkioxari, P. Dollár, and R. Girshick. Mask r-cnn. In *Proceedings of the IEEE international conference on computer vision*, pages 2961–2969, 2017.
- [9] K. He, X. Zhang, S. Ren, and J. Sun. Deep residual learning for image recognition. In *Proceedings of the IEEE conference on computer vision and pattern recognition*, pages 770–778, 2016.
- [10] Z. Huang, L. Huang, Y. Gong, C. Huang, and X. Wang. Mask scoring r-cnn. In *Proceedings of the IEEE Conference on Computer Vision and Pattern Recognition*, pages 6409–6418, 2019.
- [11] E. Insafutdinov, L. Pishchulin, B. Andres, M. Andriluka, and B. Schiele. Deeppercut: A deeper, stronger, and faster multi-person pose estimation model. In *European Conference on Computer Vision*, pages 34–50. Springer, 2016.
- [12] T.-Y. Lin, P. Dollár, R. Girshick, K. He, B. Hariharan, and S. Belongie. Feature pyramid networks for object detection.

- In *Proceedings of the IEEE conference on computer vision and pattern recognition*, pages 2117–2125, 2017.
- [13] T.-Y. Lin, P. Goyal, R. Girshick, K. He, and P. Dollár. Focal loss for dense object detection. In *Proceedings of the IEEE international conference on computer vision*, pages 2980–2988, 2017.
 - [14] T.-Y. Lin, M. Maire, S. Belongie, J. Hays, P. Perona, D. Ramanan, P. Dollár, and C. L. Zitnick. Microsoft coco: Common objects in context. In *European conference on computer vision*, pages 740–755. Springer, 2014.
 - [15] A. Newell, Z. Huang, and J. Deng. Associative embedding: End-to-end learning for joint detection and grouping. In *Advances in neural information processing systems*, pages 2277–2287, 2017.
 - [16] A. Newell, K. Yang, and J. Deng. Stacked hourglass networks for human pose estimation. In *European conference on computer vision*, pages 483–499. Springer, 2016.
 - [17] X. Nie, J. Feng, J. Zhang, and S. Yan. Single-stage multi-person pose machines. In *Proceedings of the IEEE International Conference on Computer Vision*, pages 6951–6960, 2019.
 - [18] G. Papandreou, T. Zhu, L.-C. Chen, S. Gidaris, J. Tompson, and K. Murphy. Personlab: Person pose estimation and instance segmentation with a bottom-up, part-based, geometric embedding model. In *Proceedings of the European Conference on Computer Vision (ECCV)*, pages 269–286, 2018.
 - [19] L. Pishchulin, E. Insafutdinov, S. Tang, B. Andres, M. Andriluka, P. V. Gehler, and B. Schiele. Deepcut: Joint subset partition and labeling for multi person pose estimation. In *Proceedings of the IEEE conference on computer vision and pattern recognition*, pages 4929–4937, 2016.
 - [20] J. Redmon, S. Divvala, R. Girshick, and A. Farhadi. You only look once: Unified, real-time object detection. In *Proceedings of the IEEE conference on computer vision and pattern recognition*, pages 779–788, 2016.
 - [21] G. Rogez, P. Weinzaepfel, and C. Schmid. Lcr-net++: Multi-person 2d and 3d pose detection in natural images. *IEEE transactions on pattern analysis and machine intelligence*, 2019.
 - [22] K. Sun, B. Xiao, D. Liu, and J. Wang. Deep high-resolution representation learning for human pose estimation. In *Proceedings of the IEEE Conference on Computer Vision and Pattern Recognition*, pages 5693–5703, 2019.
 - [23] K. Sun, B. Xiao, D. Liu, and J. Wang. Deep high-resolution representation learning for human pose estimation. In *Proceedings of the IEEE Conference on Computer Vision and Pattern Recognition*, pages 5693–5703, 2019.
 - [24] M. Sun and S. Savarese. Articulated part-based model for joint object detection and pose estimation. In *2011 International Conference on Computer Vision*, pages 723–730. IEEE, 2011.
 - [25] X. Sun, B. Xiao, F. Wei, S. Liang, and Y. Wei. Integral human pose regression. In *Proceedings of the European Conference on Computer Vision (ECCV)*, pages 529–545, 2018.
 - [26] Z. Tian, H. Chen, and C. Shen. Directpose: Direct end-to-end multi-person pose estimation. *arXiv preprint arXiv:1911.07451*, 2019.
 - [27] Z. Tian, C. Shen, H. Chen, and T. He. Fcos: Fully convolutional one-stage object detection. In *Proceedings of the IEEE International Conference on Computer Vision*, pages 9627–9636, 2019.
 - [28] Z. Yang, S. Liu, H. Hu, L. Wang, and S. Lin. Reppoints: Point set representation for object detection. In *Proceedings of the IEEE International Conference on Computer Vision*, pages 9657–9666, 2019.